Remote sensing indices for monitoring land degradation in a semiarid to arid basin in Jordan

Jawad Al-Bakri[a] (corresponding author), Hani Saoub[b], William Nickling[c], Ayman Suleiman[a], Mohammad Salahat[d], Saeb Khresat[e], Tarek Kandakji[a]

[a]Dept. of Land, Water and Environment, Faculty of Agriculture, University of Jordan, Amman, Jordan. e-mail: jbakri@ju.edu.jo, Tel. +962-6-5355000/ext.22444, Fax. +962-6-5300806: [b]Dept. of Horticulture and Crop Science, Faculty of Agriculture, University of Jordan, Amman, Jordan: [c]Wind Erosion Laboratory, Dept. of Geography, University of Guelph, Toronto, Canada: [d]Dept. of Natural Resources & Environment, Hashemite University, Zarqa, Jordan: [e]Dept. of Natural Resources & Environment, Jordan University of Science & Technology, Irbid, Jordan.

ABSTRACT

Spectral reflectance for soils and vegetation of the Yarmouk basin were correlated with surficial soil properties and vegetation biomass and cover. The overall aim of the study was to identify bands suitable for assessing soil and vegetation as indices for land degradation and desertification. Results showed that vegetation was well separated from soils in the shortwave infrared wavelength at 1480 nm. For most sites, the differences in the bandwidths (in the range of 8.5 nm to 90 nm) did not improve the differentiation of vegetation types. For all wavelengths, stronger correlation values (maximum R^2 = 0.85) were obtained for vegetation cover when compared with biomass (maximum R^2 = 0.54). Soil spectral reflectance tended to increase with salinity, with maximum correlations obtained in the blue wavelengths (470±10 nm, 485±90 nm), followed by green and the NIR bands, where R^2 values were around 0.60. Comparing results from radiometer measurements with results obtained from ASTER image bands showed that correlations tended to decrease with decreased spatial resolution for the investigated soil properties. For all wavelengths, spectral reflectance of degraded soils was higher than that for natural vegetation and irrigated crops with partial surface cover. Results of the study showed that the use of remote sensing indices related to vegetation cover and soil salinity would be recommended to map the extent of land degradation in the study area and similar environments. However, spectral unmixing should be applied to improve the correlations between satellite remote sensing data and surficial soil properties.

Keywords: Spectral reflectance, remote sensing indices, spectral unmixing, Jordan.

1. INTRODUCTION

Monitoring land degradation in arid and semiarid areas is crucial for assessing the levels of desertification and loss of land and water resources. Although monitoring and assessment of desertification and land degradation to support decision-making in land and water management is seen as a first priority theme[1], quantitative maps are still lacking in many developing countries due to lack of financial and technical resources. Remote sensing technology can contribute to the international efforts in mapping the extent of land degradation and desertification by providing multispectral data for large areas at reasonable costs. Also, it would provide spatially explicit and up-to-date information related to biophysical indicators of land degradataion[2]. The improvement in spectral, spatial and temporal resolutions would enhance the scientific communities to apply remote sensing for mapping land degradation and for assessing changes in soil and land resources.

Application of remote sensing for assessing and monitoring land degradation is mainly related to spectral reflectance of soils and vegetation. The most important interaction of soils and electromagnetic radiation is in the range of 0.3 to 3 μm. In arid and semiarid areas, spectral reflectance of soil is mainly controlled by the dominant particle size and the content of minerals, including accumulated salts. Generally speaking, spectral reflectance of soils increases with increasing

Earth Resources and Environmental Remote Sensing/GIS Applications III, edited by Daniel L. Civco, Manfred Ehlers, Shahid Habib, Antonino Maltese, David Messinger, Ulrich Michel, Konstantinos G. Nikolakopoulos, Karsten Schulz, Proc. of SPIE Vol. 8538, 853810 • © 2012 SPIE • CCC code: 0277-786/12/$18 • doi: 10.1117/12.974333

wavelength in the visible and near infrared portions of spectrum[3]. In arid and semiarid areas, the level of spectral reflectance of soil is also altered by clay content and the presence of surface crust[4]. On the other hand, spectral reflectance of vegetation is mainly controlled by pigmentation, water content and leaf structure. The most important wavelengths of the electromagnetic radiation for detecting vegetation are the red and the near infrared (NIR). The combinations of the two bands, known as vegetation indices, are usually used to monitor plant parameters related to vegetation biophysical quantities[5,6]. The red-NIR vegetation indices are also used to assess vegetation conditions as related to different stresses[7,8,9].

The use of remote sensing for monitoring land degradation in arid and semiarid areas is facilitated by the sparse vegetation, the clear skies, the shortage of rainfall and the low soil moisture. The first few centimeters of soils in these areas are the most fertile and most susceptible to erosion by water and wind. Therefore, changes in soil surface properties can provide good indicators of land degradation or rehabilitation, as well as important information for assessing the problems of climate change and loss of biodiversity[10,11]. Detection of changes in soil surface properties is possible through the use of empirical models that correlate spectral information of a representative set of samples (calibration set) with these properties[12]. This will require research studies to cover the variety of soil types existing in arid and semiarid environments. Also, the temporal changes in vegetation state and in the soil/rock signature emphasize the need for more research in the use of multispectral imagery from airborne or spaceborne sensors for detecting and monitoring the temporal dynamics of soil and natural vegetation in these environments[12]. This study aims to identify the multispectral bands that can be deployed in remote sensing indices for detecting and monitoring surficial soil properties and vegetation in a semiarid to arid environment in Jordan. The ultimate output from the study shall serve the purpose of monitoring land degradation and desertification in the country.

2. METHODOLOGY

2.1 Study area

The study was carried out in the north of Jordan in an area that comprises the upstream parts of the Zarqa and Yarmouk Rivers basins (Figure 1). The two basins are the main sources of surface water for the country which is among the four driest countries in the world, with a per capita renewable water share of 145 m^3 per year, far below the international water poverty line of 500 m^3 per year[14]. The study area, covers approximately 1400 km^2, is characterized by a semiarid to arid Mediterranean climate with high rainfall variability. The climate of this Mediterranean study area is characterized by cool rainy winters and hot dry summers. Mean annual rainfall varies between 450 mm in the west to less than 150 mm in the east. The rainy season starts in November and ends by early May. The annual potential evaporation ranges from 1400 to 2200 mm/year. The average temperature range is 22-31 °C in summer and 8.0-15 °C in winter.

The study area is extremely important to Jordan in that it is the main source of surface water at the present time that discharges through the Yarmouk and Zarqa Rivers. Due to construction of more than 25 dams within the Syrian parts of the Yarmouk basin and the heavy extraction of groundwater in Jordan and Syria, the total flow of the Yarmouk River has dropped from 430 MCM before 1970 to less than 260 MCM in the 1980s and early 1990s[15]. On the other hand, the heavy withdrawal of groundwater in the Zarqa River basin has resulted in a base flow reduction from 5 m^3/s to less than 1 m^3/s.

A wide range of soil types, reflecting the wide range of its physical characteristics, exists in the study area. In the western parts, the dominant soil subgroup is typic xerochrepts with low content of carbonates and high content of clay. In eastern parts, calcixerollic and lithic subgroups are dominant, with high contents of carbonates and silt fraction. Deep vertisols are dominating the area between Irbid and Ramtha cities on the undulating plateau and in some wadi floors[16]. Rainfed and irrigated agriculture are practiced in this basin. In the western parts, rainfed field crops, olives and vegetables are grown. The eastern parts of the study area are cultivated with barley and are used as open rangelands for grazing. Irrigation is also practiced in the study area, with ground water as the main irrigation water source. The dominant aspects of land degradation in the eastern parts of the study area are the high rates of erosion by wind and water, the substantial accumulation of calcareous silt on the soil surface, degradation of natural vegetation and the low density of plant cover caused by overgrazing and poor rainfall distribution.

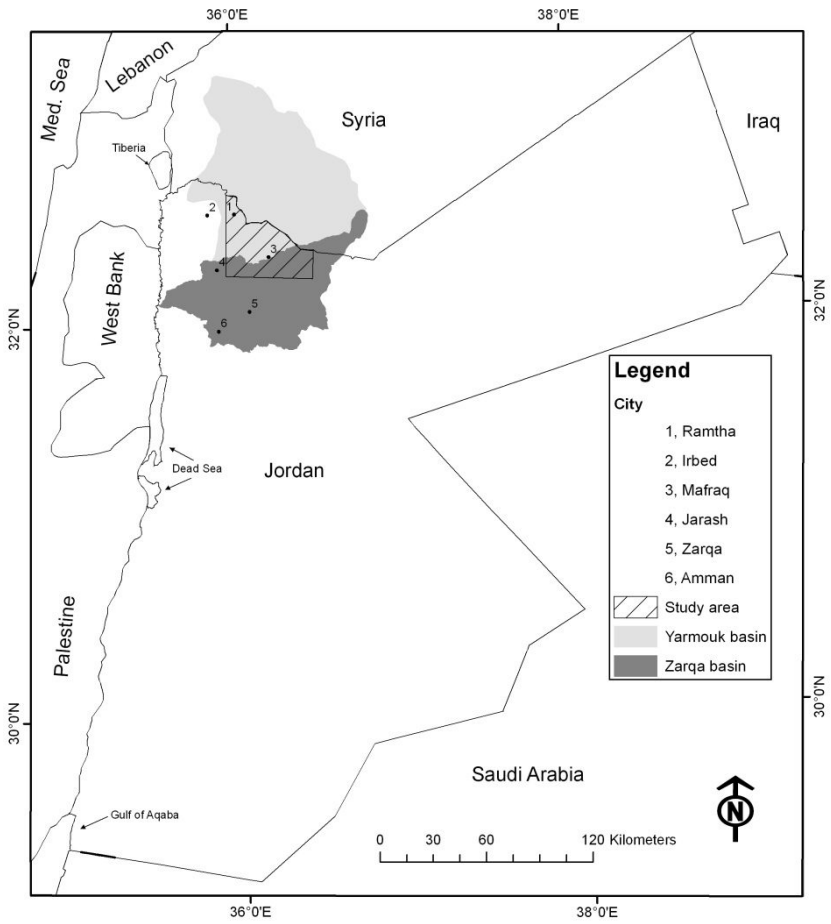

Figure 1. Location of the study area.

2.2 Spectral reflectance measurements and data

The study was based on recording soil spectral reflectance in the field and collecting soil and vegetation samples from the same locations of radiometer measurements. To achieve this goal, the study team carried out field excursions within the study area and collected measurements from locations that were separated by 3 to 4 km. The exact position of sampling locations was recorded by a global positioning system (GPS). In total, the team sampled 106 locations that were distributed as uniformly as possible to cover different land cover types, with exception to urbanized areas. During the surveys, soil surface spectral reflectance was measured by a multispectral radiometer (CROPSCAN MSR16R) with 16 bands covering the visible, NIR and shortwave infrared (SWIR) parts of the electromagnetic spectrum. The radiometer was attached to an aluminum pole to take measurements at a constant height of 2.5 m. This enabled the team to record spectral reflectance for a circular ground sampled interval (GSI) of $5m^2$. In terms of spatial resolution, this would be equivalent to a pixel size of 2.2 m. Characteristics and descriptions of each sampling location were recorded by the survey team. The description was designed to follow the specific objectives of the study and it included the land use type, vegetative cover type and percentage, crust presence, rock type and percentage, slope, erosion status and anthropogenic activities near the site. Quantitative data on surface covers and the percentage of each, the type of soil, rock and vegetation was recorded for the GSI and for area dimensions of 15 by 15 m and 30 by 30 m. This was made to enable comparisons between data from radiometer and medium resolution satellite images. Spectral reflectance measurements were also made for each cover type by adjusting the height of measurements in order to collect data necessary for applying spectral unmixing to the end members of each sampled location.

In order to compare results from the radiometer with spectral reflectance recorded from space, a satellite image of the Advanced Spaceborne Thermal Emission and Reflection Radiometer (ASTER) was obtained and processed to extract

spectral reflectance data for the same sampled locations. The image covered an area of 60 by 60 km and was acquired in early May. The image was geometrically corrected by ground control points (GCP's) collected by the GPS. An absolute radiometric correction was carried out to convert digital numbers (DN) to spectral reflectance using measurements collected by the multispectral radiometer for reference objects (Paved roads and floors of quarries). Following the stage of radiometric correction, values of reflectance were extracted for pixels where soil samples were collected.

2.3 Collection and analysis of soil samples

For each location, a composite soil sample was collected from the upper most top soil surface with a hand shovel. The samples were prepared for standard chemical and physical analysis, which included soil salinity (EC, electrical conductivity) and sodium content measured for the soil paste, particle size distribution (sand, silt, and clay) using the sedimentation technique, organic matter (OM) content through chemical oxidation, carbonate content ($CaCO_3$) using the calcimeter.

2.4 Sampling of vegetation

Sampling was mainly carried out for rainfed barley, which is the most important crop that is cultivated to support livestock with grain and straw in wet years and with straw in the dry years. Ground surveys were carried out during April-May of years 2010 and 2011 to measure biomass and cover of barley and to record spectral reflectance of this crop. The aim was to assess the levels of productivity and to correlate above ground biomass and cover of barley with spectral reflectance, so that remote sensing indices for this important bio-indicator would be identified. For each location, three 30-m transects were laid out randomly at angle of 60 degrees from one another, where transects meet at the same center point. Along each transect, five quadrates were sampled for plant biomass and cover. The team collected plant material by cutting plants from 1.0 m^2 quadrates, to soil surface using sickles. Plant cover was visually estimated by the team and recorded as percent. In each field, quadrates were randomly allocated and spectral reflectance was measured using the multispectral radiometer prior to plant cutting. Plant material was placed in paper bags, tagged and then placed in the oven for drying. The dry weight for the total biomass (above ground) was recorded. In total, the numbers of sampled fields of barley were 28 and 19 for years 2010 and 2011, respectively.

2.5 Analysis of data

Data of spectral reflectance, from both radiometer and from ASTER, was correlated with soil and vegetation data using linear regression analysis. The procedure was applied on data with and without spectral unmixing. The procedure of spectral unmixing was carried out to eliminate the effect of vegetation and rocks on soil surface reflectance inside the sampled pixel as follows[17]:

$$\rho_i = \sum_{j=1}^{n} \left(\rho_{ij}.F_i\right) + E_i \qquad (1)$$

Where:
$i = 1,\ldots, m$ (number of bands);
$j = 1,\ldots, n$ (number of end-members, pure objects of soil, rock and vegetation);
ρ_i = spectral reflectance of the ith spectral band of a pixel or GSI;
ρ_{ij} = known spectral reflectance of the jth component;
F_j = the fraction coefficient of the jth component within the pixel;
E_i = error for the ith spectral band.

3. RESULTS AND DISCUSSION

3.1 Spectral reflectance curves

Results showed that soils and vegetation of the study area were distinguished in terms of their spectral reflectance (Figure 2). Without spectral unmixing, crusted soils would have higher spectral reflectance than vegetation in all investigated wavelengths (Figure 2a). Although many points could be discussed in terms of spectral reflectance for the different land cover types, however, the focus would be on bands that could be utilized for monitoring land degradation. The distinguished spectral profiles of the different soil types and the changes in spectral reflectance with increased level of degradation would be two important points to consider. Comparing the spectral profile of a vertisol in the western part of the study area with the profiles of two aridic soils (Suborders of Cambids and Calcids) would indicate that soils under aridic soil moisture regime would have higher spectral reflectance than vertisols with xeric soil moisture regime. The

degraded soils in the eastern parts of the study area were characterized by the presence of surface crust that had high reflectance in the visible to infrared parts of the electromagnetic spectrum. Therefore, we would expect that land degradation and desertification would increase soil spectral reflectance in all visible to NIR wavelengths.

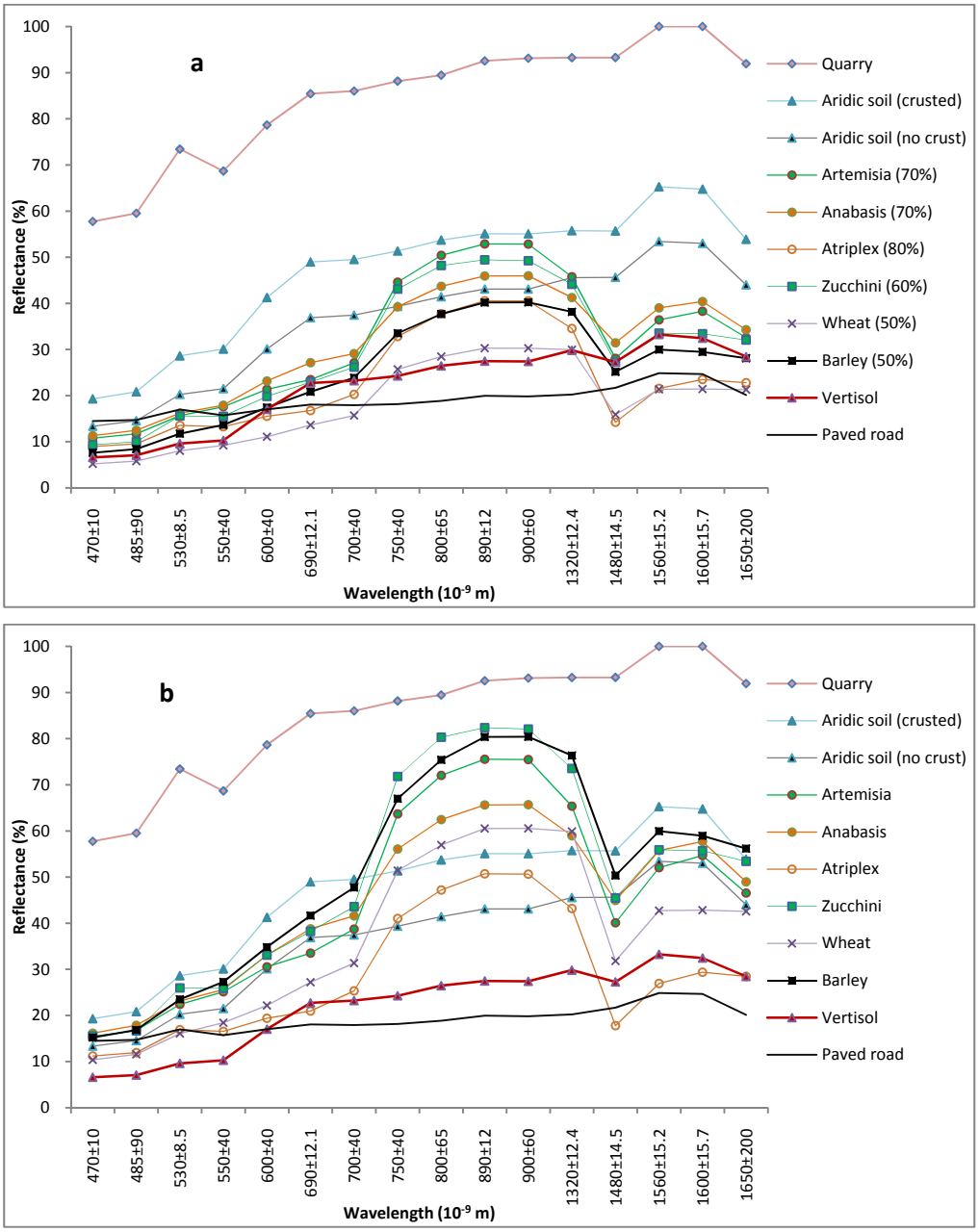

Figure 2. Spectral reflectance for different land covers in the study area before (a) and after (b) applying spectral unmixing.

Results from radiometer measurements also showed aridic soils with surface crust would have higher reflectance than vegetation with partial cover of the soil surface. The differentiation between vegetation and soils, therefore, would be difficult and would require the use of the SWIR (1480 nm) in remotes sensing indices. In terms of NIR bands, no differences were observed in soil spectral reflectance and the curve of spectral reflectance was nearly flat, while vegetation tended to have the highest reflectance around the 900 nm wavelength. Results also showed that the differences in the bandwidths (in the range of 8.5 nm to 90 nm) did not improve the differentiation of vegetation types. The use of spectral unmixing improved the separation of the different vegetation types from soils, particularly in the NIR (Figure 2b). Only the *Atriplex spp*. tended to have lower spectral reflectance than crusted soils in the NIR wavelength.

This could be attributed to the nature of this vegetation type as its relatively large canopy was containing more dry branches than other natural vegetation types.

3.2 Spectral reflectance and soil properties

Results showed variations in soil surface properties among the sampled locations (Table 1). Generally, most of the sampled locations were characterized by low organic matter content and high contents of carbonate, particularly for locations in the eastern part of the study area. Soil salinity was relatively high in some locations and reached 91 dS/m for a salinized field that was abandoned after being irrigated. Soil pH was characterized by low variations among the different samples as the soils were calcareous with medium to high contents of carbonate. In terms of particle size distribution, most of the sampled locations were characterized by a medium texture with a relatively high silt fraction. Results from linear regression analysis showed that spectral reflectance was significantly correlated with soil salinity, clay, sand and silt (Table 2).

Table 1. Summary of soil analysis results for the collected soil samples.

	$CaCO_3$ (%)	OM (%)	Clay (%)	Silt (%)	Sand (%)	ECe (dS/m)	pH	Na (ppm)
Mean	24.8	1.5	32.8	54.7	12.5	4.1	8.3	417
Minimum	2.5	0.8	19.0	32.0	4.3	0.4	7.0	10
Maximum	49.1	3.0	62.5	66.8	23.5	90.9	8.7	7850
Std*	9.4	0.4	11.4	9.0	4.8	10.8	0.3	1206
CV** (%)	37.9	24.0	34.6	16.5	38.0	264.7	3.2	289

*, **: Standard deviation and coefficient of variation, respectively

Table 2. Coefficient of determination (R^2) for the different correlations between soil and vegetation parameters and spectral reflectance (ρ), recorded by the radiometer, after applying spectral unmixing.

Band	Wavelength (nm)	EC vs. ρ	Na vs. ρ	Clay vs. ρ	Silt vs. ρ	Sand vs. ρ	Biomass vs. ρ	Cover vs. ρ
B1	470±10	0.77	0.66	0.52	0.17	0.42	0.45	0.73
B2	485±90	0.74	0.61	0.52	0.17	0.43	0.47	0.75
B3	530±8.5	0.43	0.28	0.58	0.23	0.42	0.54	0.68
B4*	550±40	0.63	0.51	0.53	0.15	0.46	0.47	0.74
B5	600±40	0.64	0.53	0.48	0.15	0.40	0.47	0.81
B6**	690±12.1	0.58	0.45	0.47	0.15	0.39	0.46	0.85
B7	700±40	0.58	0.44	0.47	0.15	0.38	0.46	0.83
B8	750±40	0.58	0.44	0.49	0.16	0.40	ns	ns
B9***	800±65	0.59	0.46	0.48	0.18	0.36	ns	ns
B10	890±12	0.61	0.46	0.48	0.18	0.37	ns	0.24
B11	900±60	0.61	0.46	0.48	0.17	0.37	ns	0.23
B12	1320±12.4	0.36	0.23	0.55	0.24	0.38	0.37	0.40
B13	1480±14.5	ns	ns	0.42	0.19	0.29	0.39	0.82
B14	1560±15.2	0.60	0.46	0.38	ns	0.34	0.43	0.80
B15	1600±15.7	0.54	0.42	0.32	ns	0.34	0.43	0.78
B16	1650±200	0.51	0.37	0.48	0.17	0.37	0.42	0.77

*, **, ***: The range of ASTER bands 1, 2 and 3, respectively.
SEYX: standard error of y predicted by x.
ns: not significant at 0.05 P-level.

Soil salinity had significant correlation with spectral reflectance in the visible, near infrared (NIR), and shortwave infrared (SWIR), except the 1480 nm wavelength where no correlation was observed. The maximum correlations were obtained in the blue wavelengths (B1 and B2), followed by green (B4 and B5) and the NIR bands, where R^2 values were around 0.60, after applying spectral unmixing. All SWIR bands, except B13, were significantly correlated with soil salinity, with slightly higher correlation in B14 (narrow wavelength) than B16 (broad wavelength). These results showed that it would be possible to detect salinized soils from remote sensing data using a combination of one or more of the remote sensing bands, particularly the green (B4 and B5), the NIR (B10 and B11), and the SWIR (B14). Although reflectance in blue bands (B1 and B2) was more correlated with soil salinity than the other bands, however, both wavelengths would be affected by atmospheric interactions (Rayleigh scattering). This would limit their use in monitoring soil salinity from air-borne systems of remote sensing. The same trends of correlations were observed for Na, which seemed to be the main cause of soil salinization in the study area.

Comparing the results from radiometer with results from ASTER bands showed that correlations decreased with increased pixel size. Spectral reflectance derived from ASTER had significant ($P < 0.05$) linear relationship with soil salinity in the green, red, and NIR bands with relatively low R^2 values when compared to radiometer results for the same bands of ASTER (Figure 3). These results could be attributed to the increased heterogeneity among the end-members within the GSI at the level of 15 m when compared with the GSI of 2.2 m.

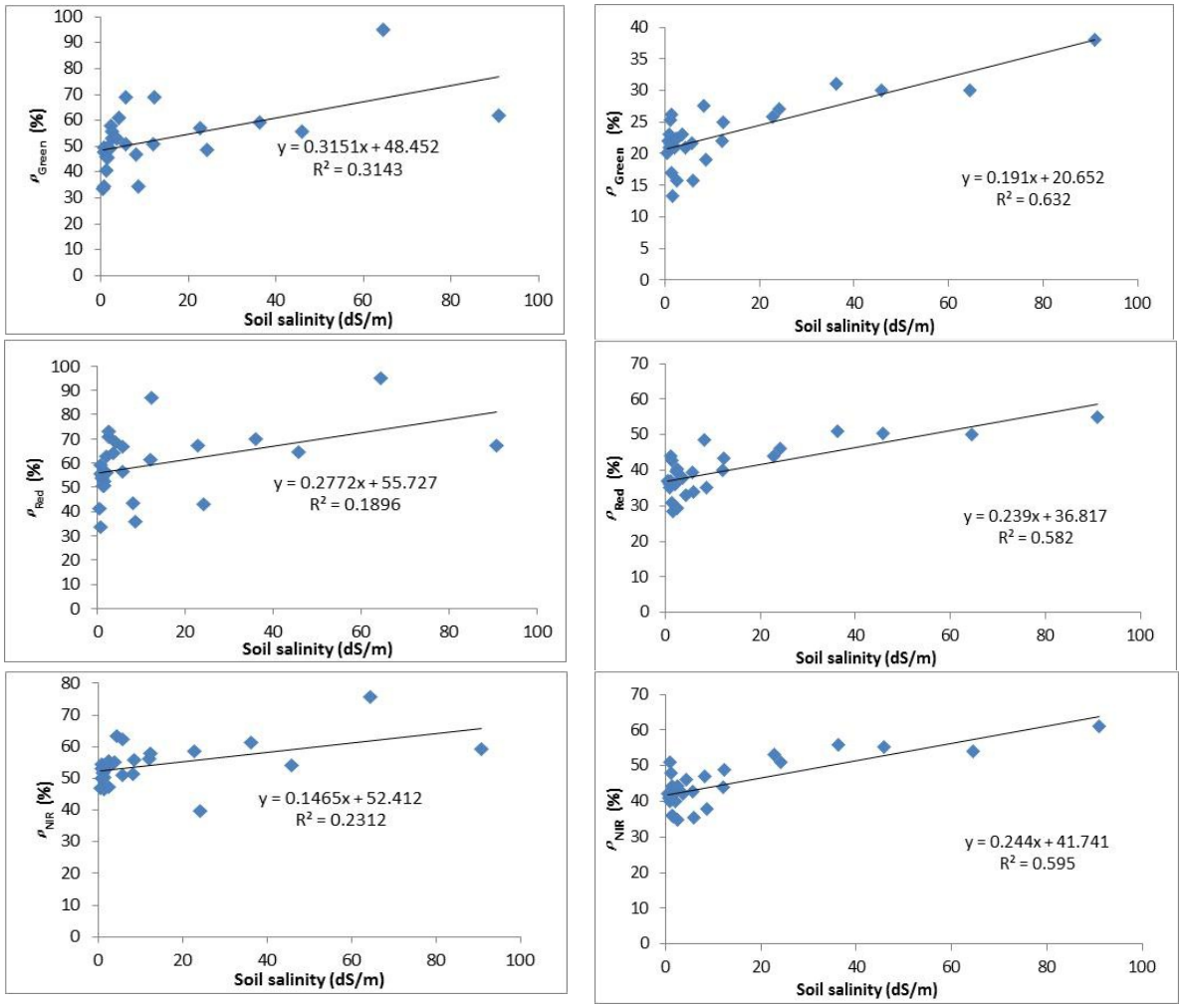

Figure 3. Relationships between soil salinity and spectral reflectance derived from ASTER (Left) and the multispectral radiometer measurements (Right).

Results showed that spectral reflectance was more correlated with clay and sand than with silt. Using linear regression, the maximum correlation with visible bands was in the green wavelength, while the maximum correlation in the SWIR was at the 1320 nm (Table 2). Generally, higher R^2 values were obtained for clay than for sand in all bands, except B15. A positive relationship was observed between sand and spectral reflectance. Oppositely, soil spectral reflectance decreased with increasing clay content. For all bands, the values of R^2 improved when a power relationship was used to correlate spectral reflectance with soil content of sand. For band 4, the maximum R^2 increased from 0.46 for the linear relationship and reached 0.56 for the power relationship.

3.3 Spectral reflectance and vegetation parameters

Results of vegetation mapping showed variations in vegetation biomass and cover across the study area and between years 2010 and 2011. Plant cover ranged from 5 to 100% and from 20 to 100% in 2010 and 2011, respectively (Table 3). Biomass levels were also higher in year 2011 (Season 2010/2011) than in year 2010 (Season 2009/2010). This could be attributed to the higher rainfall in season 2010/2011 than in season 2009/2010. In both seasons, however, variations in biomass and cover were observed. This was expected in the study area which was characterized by frequent droughts and relatively low rainfall amounts in the last two decades[18]. Analysis of data also showed that levels of biomass production in the east were extremely low when compared to the northwest of the study area. In season 2010/2011, for example, the biomass of barley was 241 kg/ha in the south east, near Mafraq City, and reached 981 kg/ha in the northeast of the study area. On the other hand, the levels of biomass in the western parts ranged from 695 to 4400 kg/ha. The main reason behind these differences was the rainfall variation. During maturity stage, the biomass ranged from 110 kg/ha (In the far eastern sampled location) up to 300 kg/ha in the west. Meanwhile, during late stage of growth, the biomass ranged from 390 to 4400 kg/ha. Meanwhile, the level of biomass production for irrigated barley reached 7755 kg/ha in the late stage of growth. These results could reflect the impact of rainfall variation and the management practices across the study area.

Table 3. Summary of plant cover and biomass of rainfed barley for the sampled locations inside the study area.

	Season 2009/2010		**Season 2010/2011**	
	Biomass (kg/ha)	**Cover (%)**	**Biomass (kg/ha)**	**Cover (%)**
Mean	1529	50	2339	43
Minimum	110	5	241	20
Maximum	3800	100	5510	100
Std*	892	31	1637	24
CV** (%)	58	63	70	57
Seasonal Rainfall (mm)				
Irbid	413		458	
Ramtha	194		216	
Mafraq	147		113	

*, **: Standard deviation and coefficient of variation, respectively

Regression analysis (Table 2) showed that vegetation cover was significantly correlated with most spectral bands. The highest correlation was in the red band with wavelength of 690±12.1 nm, followed by the NIR band with a wavelength of 700±40 nm. The two SWIR bands of 1480 and 1560 nm were also highly correlated with vegetation cover. These results indicated that the combinations of the above wavelengths would provide good indices for monitoring vegetation cover of barley. The most commonly used and known index for this purpose is the normalized difference vegetation index (NDVI), which is calculated as the difference between the NIR and red reflectance values normalized with their sum[6,19]. In this study, different combinations of the NIR and red were correlated with the plant cover of barley. Results showed that the NDVI from the combinations of 890±12 or 900±60 nm NIR wavelengths and any of the three red bands (600±40, 690±12.1, 700±40) were significantly correlated with the cover. The maximum R^2 for the cover-NDVI relationship reached 0.86 for the combination of NIR of 900±60 and the red band of 600±40.

Significant correlations between biomass and spectral reflectance were observed in 12 out of the 16 bands. Values of R^2, however, were lower for the biomass-NDVI relationships when compared to the cover-NDVI realtionships. The maximum R^2 for the biomass-NDVI relationship reached 0.34. This could be attributed to the different cultivars of barley, which would differ in biomass production for the same levels of vegetation cover.

All of the above results were obtained from the radiometer measurements, at the level of GSI of 2.2 m. For the ASTER image, the biomass-NDVI relationship was not significant while the cover-NDVI relationship had an R^2 value of 0.62. These results would recommend the use of vegetation cover as a remotely sensed parameter for monitoring desertification in the study area. Meanwhile, monitoring of biomass of the study area from remote sensing data would require more samples with more data on crops and their management.

4. CONCLUSIONS

The use of spectral reflectance to predict surficial soil properties and vegetation parameters in the arid and semiarid environments showed that some remote sensing bands could provide useful tools for mapping land degradation. The most important soil properties that were correlated with visible, NIR and SWIR bands were soil salinity and soil texture. The wavelengths that had the maximum correlations with salinity were the blue (470±10 nm, 485±90 nm), followed by green and the NIR bands. Both of clay and sand were significantly correlated with all bands, with maximum correlations obtained in the green wavelengths. In terms of vegetation monitoring, the use of the NIR and red bands would provide good indices for this purpose, particularly for plant cover. Spectral reflectance curves, however, showed that aridic soils, particularly with surface crusts, would have higher reflectance in all visible to infrared bands. Differentiating these soils from vegetation would require the use of spectral unmixing to improve mapping and monitoring of these important biophysical indicators of land degradation.

ACKNOWLEDGMENTS

This research and publication were supported by the NATO's Science for Peace Program, project SfP-983368 (2009-2012) "Assessment and monitoring of desertification in Jordan using remote sensing and bioindicators". The authors acknowledge Azzam Ananbeh and Ibrahim Farhan from University of Jordan for their efforts in field surveys. Thanks are extended to Ze'ev Gedalof, University of Guelph-Canada, Catherine Champagne, Agriculture and Agri-Food-Canada, for their assistance and advice in collecting soil and vegetation measurements by the radiometer.

REFERENCES

[1] UNCCD (United Nation Convention to Combat Desertification), "The UNCCD 1st Scientific Conference: Synthesis and recommendations and COPs-CST 9th session," Buenos Aires, 22-25 September 2009, UNCCD, (2009).
[2] Röder, A. and Hill, J., [Recent Advances in Remote Sensing and Geoinformation Processing for Land Degradation Assessment], ISPRS Book Series, ISBN: 978-0415397698, Taylor & Francis, London, pp.418 (2009).
[3] Asrar, G., [Theory and applications of optical remote sensing], John Wiley and Sons, New York, (1989).
[4] Eshel, G., Levy, G. J. and Singer, M. J. "Spectral Reflectance Properties of Crusted Soils under Solar Illumination," Soil Sci. Soc. Am. J. 68 (6), 1982-1991(2004).
[5] Jiang, Z., Huete, A.R., Li, J. and Qi, J. "Interpretation of the modified soil-adjusted vegetation index isolines in red-NIR reflectance space," J. Appl. Remote Sens. 1, 013503 (2007).
[6] Papadavid, G., Hadjimitsis, D., Toulios, L. and Michaelides, S. "Mapping potato crop height and leaf area index through vegetation indices using remote sensing in Cyprus," J. Appl. Remote Sens. 5, 053526 (2011).
[7] Vohland, M. "Using imaging and non-imaging spectroradiometer data for the remote detection of vegetation water content," J. Appl. Remote Sens. 2, 023520 (2008).
[8] Helmi Z. M. Shafri, M. Anuar, I. and Saripan, M.I. "Modified vegetation indices for Ganoderma disease detection in oil palm from field spectroradiometer data," J. Appl. Remote Sens. 3, 033556 (2009).

[9] Hunt, E.R., Daughtry, C.S.T., Kim, M.S. and Williams, A.E.P. "Using canopy reflectance models and spectral angles to assess potential of remote sensing to detect invasive weeds," J. Appl. Remote Sens. 1, 013506 (2007).
[10] Cowie, A. L., Penman, T. D., Gorissen, L., Winslow, M. D., Lehmann, J., Tyrrell, T. D., Twomlow, S., Wilkes, A., Lal, R., Jones, J. W., Paulsch, A., Kellner, K. and Akhtar-Schuster, M. "Towards sustainable land management in the drylands: Scientific connections in monitoring and assessing dryland degradation, climate change and biodiversity, " Land Degradation & Development 22, 248–260 (2011).
[11] Ustin, S.L., Palacios-Orueta, A., Whiting, M.L., Jacquemoud, S. and Li, L., "Remote sensing based assessment of biophysical indicators for land degradation and desertification," In: [Recent Advances in Remote Sensing and Geoinformation Processing for Land Degradation Assessment] (Roeder A. & Hill J., Eds), ISPRS Book Series, ISBN: 978-0415397698, Taylor & Francis, pp. 15-44 (2009).
[12] Ben-Dor, E., Patkin, K., Banin, A. and Karnieli, A. "Mapping of several soil properties using DAIS-7915 hyperspectral scanner data - a case study over clayey soils in Israel," Int. J. Remote Sens. 23(6), 1043-1062 (2002).
[13] Karnieli, A., Gabai, A., Ichoku, C., Zaady, E. and Shachak, M. "Temporal dynamics of soil and vegetation spectral responses in a semiarid environment," Int. J. Remote Sens. 23(19), 4073-4087 (2002).
[14] MWI (Ministry of Water and Irrigation, Jordan), [Water for life: Jordan's water strategy, 2008-2022], MWI, Amman, Jordan, (2009).
[15] MoEnv (Ministry of Environment, Jordan), [National Action Plan and Strategy to Combat Desertification], Ministry of Environment, Amman, Jordan, (2006).
[16] MoA (Ministry of Agriculture, Jordan), [The Soils of Jordan: Semi-detailed Level (1:50 000)], The National Soil Map and Land Use Project, Ministry of Agriculture, Amman, Jordan, (1994).
[17] Tseng, Y.H. "Spectral unmixing for the classification of hyperspectral images," Int. Arch. of Photogrammetry and Remote Sens. 33(7), 1531-1538 (2000).
[18] Al-Bakri, J.T., Suleiman, A., Abdulla, F., and Ayad, J. "Potential impacts of climate change on the rainfed agriculture of a semi-arid basin in Jordan," Phys. and Chem. of the Earth 36, 125-134 (2011).
[19] Al-Bakri, J. T. and Suleiman, A. "NDVI response to rainfall in different ecological zones in Jordan," Int. J. Remote Sens. 25(19), 3897–3912 (2004).